Nanoscale

www.rsc.org/nanoscale

Volume 2 | Number 12 | November 2010 | Pages 2493–2880

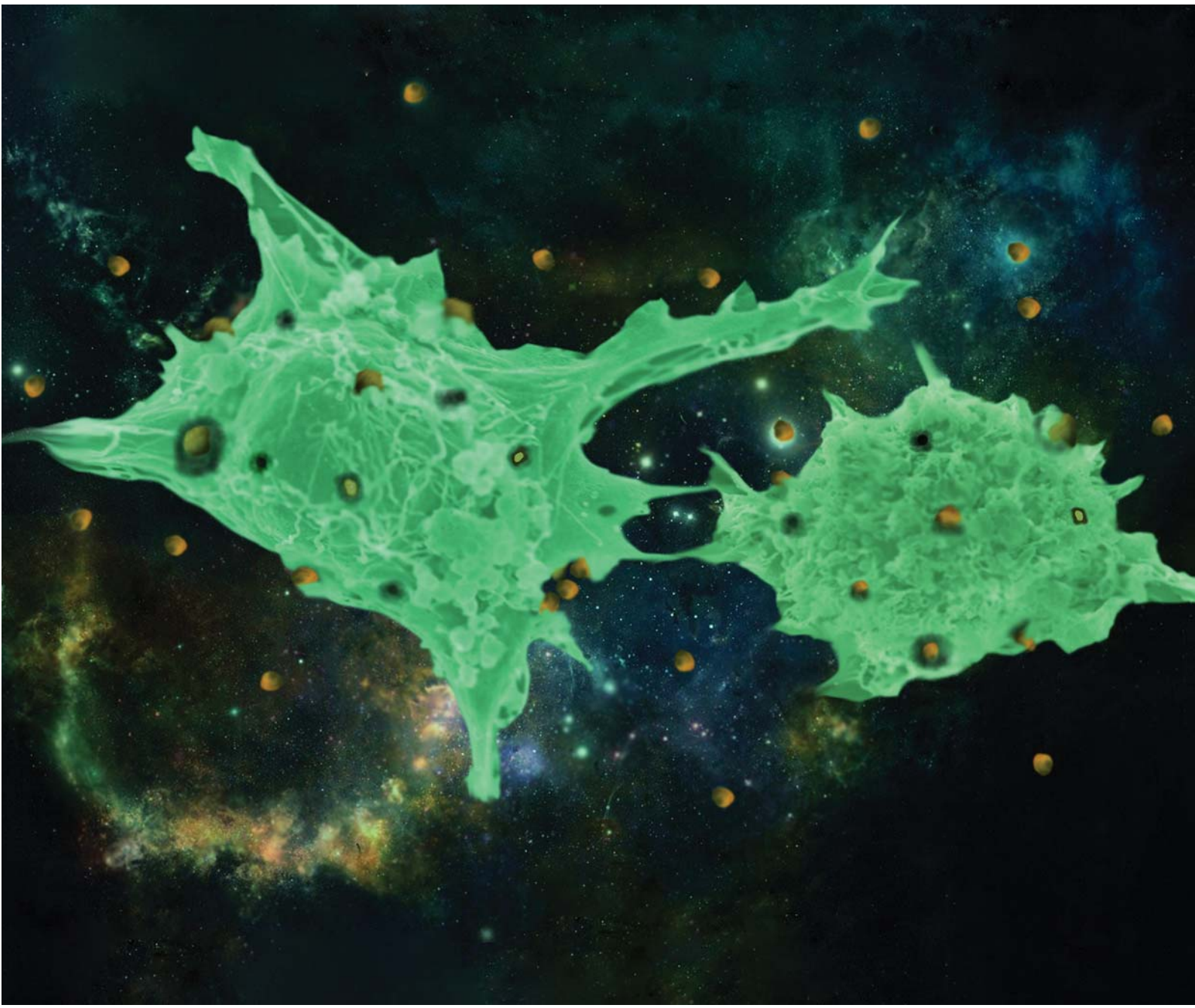

ISSN 2040-3364

RSC Publishing

COVER ARTICLE
Valiyaveettil and Teow
Active targeting of cancer cells using folic acid-conjugated platinum nanoparticles

HOT ARTICLE
Su *et al.*
Influence of surface plasmon resonance on the emission intermittency of photoluminescence from gold nano-sea-urchins

2040-3364(2010)2:12;1-V

Active targeting of cancer cells using folic acid-conjugated platinum nanoparticles

Yiwei Teow[ab] and Suresh Valiyaveettil*[ab]

Received 22nd March 2010, Accepted 2nd August 2010
DOI: 10.1039/c0nr00204f

Interaction of nanoparticles with human cells is an interesting topic for understanding toxicity and developing potential drug candidates. Water soluble platinum nanoparticles were synthesized *via* reduction of hexachloroplatinic acid using sodium borohydride in the presence of capping agents. The bioactivity of folic acid and poly(vinyl pyrrolidone) capped platinum nanoparticles (Pt-nps) has been investigated using commercially available cell lines. In the cell viability experiments, PVP-capped nanoparticles were found to be less toxic (>80% viability), whereas, folic acid-capped platinum nanoparticles showed a reduced viability down to 24% after 72 h of exposure at a concentration of 100 μg ml^{-1} for MCF7 breast cancer cells. Such toxicity, combined with the possibility to incorporate functional organic molecules as capping agents, can be used for developing new drug candidates.

Introduction

ultra-small size of nanoparticles offers unique physicochemical properties such as a large surface area to mass ratio as well as high reactivity.[1,2] In drug development, physicochemical properties such as solubility,[3] bioavailability[4] and drug targeting[5] are problems commonly encountered by medicinal chemists. With the development of nanomaterials, potential solutions for these issues are beginning to emerge. Solubility in water can be improved by introducing soluble molecules, for example poly(*N*-vinyl-2-pyrrolidone) (PVP), as capping agents on the surface of nanoparticles.[6] Bioavailability can be improved by introduction of poly(ethylene glycol) (PEG) on the surface, which reduces protein-binding and increases circulation half-life.[7] Folic acid incorporated nanoparticles have been found to target cancerous cells which over-express folate receptors on their surface.[8,9] As such, nanoparticulate drugs will be able to reach their targets more efficiently at a lower concentration. The end-result is faster drug onset and lesser side effects, both beneficial to the patient.

Currently, there are many reports on utilizing folic acid on nanocarriers for the active targeting of cancer cells over-expressing folate receptors, but information on the linking of folic acid to platinum nanoparticles (Pt-nps) by *in situ* reduction of platinic acid and investigation of toxicity have not yet been reported. We therefore demonstrate a simple method for the preparation of folic acid-capped platinum nanoparticles (Pt-FA) which have increased uptake and toxicity in cancer cells over PVP-capped nanoparticles (Pt-PVP).

Experimental

All experiments were performed in a clean atmosphere to eliminate the chances of endotoxin contamination that may interfere with the toxicity profile of the nanoparticles. Glassware used for synthesis were treated with piranha solution (3 : 1, concentrated sulfuric acid–30% hydrogen peroxide) to remove contaminants prior to reaction. Hexachloroplatinic acid hexahydrate, $H_2PtCl_6 \cdot 6H_2O$, (37.50% as Pt), sodium borohydride, $NaBH_4$ (98%) and PVP (average molecular weight 10 000) were purchased from Sigma-Aldrich; folic acid dihydrate (97%) was purchased from Alfa Aesar and used without further purification.

The selection of capping agents was done based on the stability of Pt-nps in cell culture medium. PVP- and folic acid-capped nanoparticles showed high dispersity and solubility even at high concentrations in the cell viability studies. PVP is a hydrophilic polymer which can enhance water dispersion and stability in cell culture medium. Moreover, using these two chemicals as the capping agents removed the need for the use of organic solvents or capping agents, which can be toxic to the cells.

Synthesis of platinum nanoparticles

PVP-capped platinum nanoparticles (Pt-PVP) were synthesized *via* the reduction of $H_2PtCl_6 \cdot 6H_2O$ as reported by van Rheenen *et al.* with some modifications.[10] In short, $H_2PtCl_6 \cdot 6H_2O$ (1 g) was dissolved in 19 ml ultrapure water to give 100 mM stock solution. 500 μl of the stock solution was subsequently reduced under constant stirring using $NaBH_4$ (10 mg) dissolved in 1 ml ultrapure water. Colloidal solution was then stabilized by the immediate addition of PVP (100 mg) in 10 ml ultrapure water. Final volume of the reaction mixture was kept at 50 ml. The color

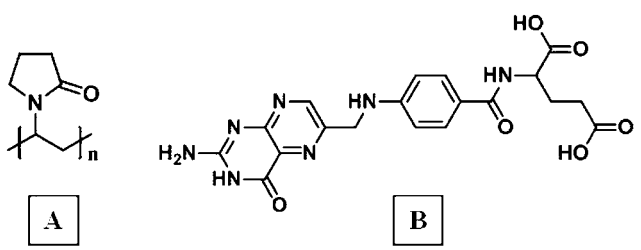

Fig. 1 Chemical structures of poly(vinyl pyrrolidone) (A) and folic acid (B).

[a]*Department of Chemistry, National University of Singapore (NUS), 3 Science Drive 3, 117543, Singapore. E-mail: chmsv@nus.edu.sg; Fax: +65 67791691; Tel: +65 65164327*
[b]*NUS Graduate School for Integrative Sciences and Engineering (NGS), National University of Singapore, 28 Medical Drive, 117456, Singapore*

of the solution changed from yellow to dark brown during the reduction process, indicating nanoparticle formation. Stirring was continued for an additional 2 h at room temperature for the reaction to complete. The procedure for the synthesis of folic acid-capped platinum nanoparticles (Pt-FA) is similar to Pt-PVP. 500 μl $H_2PtCl_6 \cdot 6H_2O$ stock solution was stirred with folic acid dihydrate (200 mg) solution for 5 min. This was subsequently reduced by adding a solution of $NaBH_4$ (2.5 mg) in a drop-wise manner. The final volume of the reaction mixture was kept at 50 ml and the final pH was adjusted to 7. The resulting solutions were centrifuged at 20 000 rpm for 45 min to obtain a pellet. The pellet was washed twice to remove traces of unbound capping agent and reducing agent. The purified solution was filtered using a 0.2 μm syringe filter to get rid of large particle aggregates. A known amount of dry solid obtained after freeze-drying was again resuspended in ultrapure water to get a stock solution. Please note that from here on, individual nanoparticles are referred as Pt-PVP and Pt-FA and in general as Pt-nps.

UV-visible spectroscopy

UV-visible measurement of Pt-nps and their capping agents were performed using a spectrophotometer (Shimadzu UV-1601PC) at room temperature.

Elemental analysis

Freeze-dried Pt-nps were analyzed for their respective elemental composition. Carbon, hydrogen and nitrogen analysis were performed using Elementar Vario Microcube. Inductively-coupled plasma analysis was used for the determination of platinum levels in digested solutions of Pt-nps. Sample preparation was done with a Milestone microwave laboratory system, while ICP was performed using Dual-view Optima 5300 DV ICP-OES. A modular ion chromatography system was used for the determination of anions such as F^- with chemical suppression. Instrumentation includes Metrohm 818 IC Pump, 820 IC Separation Center, 830 Interface, 833 IC Liquid handling Unit, 732 IC Detector and 813 Compact Autosampler.

Particle size and zeta potential measurements

The Pt-nps synthesized were observed using a JEOL 2010-F Field Emission Transmission Electron Microscope (FETEM) and a JEOL 3010 High Resolution Transmission Electron Microscope (HRTEM). For sample preparation, a dilute solution of Pt-nps dispersed in ultrapure water was placed onto a carbon-coated copper grid (400 mesh) supported on a clean filter paper and left to dry in an oven overnight. This was subsequently used for TEM. Dynamic light scattering (DLS) and zeta potential measurements were done using Malvern Zetasizer Nano-ZS.

Cell culture

Cell lines used in our study were purchased from commercial sources: HeLa and MCF7 – American Type Culture Collection, USA; IMR90 – Coriell Cell Repositories, USA. Cancer cell lines were maintained in Dulbecco's Modified Eagles Medium (DMEM, Sigma-Aldrich) supplemented with 10% fetal bovine serum (FBS Standard Quality, EU-approved origin, PAA Laboratories) and 1% penicillin–streptomycin (Gibco, Invitrogen). IMR90 at passage 18 ± 3 were maintained in Modified Eagles Medium with glutamine (MEM, PAA Laboratories) supplemented with 15% FBS, 1% each of penicillin, streptomycin, non-essential amino acids, vitamins and 2% essential amino acids (Gibco). Cells were sub-cultured at 80–90% confluence and maintained at 37 °C in a humidified incubator supplied with 5% CO_2.

CytoViva optical microscopy

This experiment was performed by growing the cell type of interest in a 24-well plate (Griener Bio-one GmbH) where one sterilized VFM coverslip (CellPath) was laid at the bottom of the well. The coverslip was washed and soaked in sterile PBS for 10 min to condition before the addition of 10 000 cells in 1 ml media, respectively, into each well. Spent media was aspirated the next day and replaced with fresh media and the cells were treated with 100 μg ml^{-1} Pt-nps for 48 h. The coverslips were removed from the wells and rinsed with fresh media before placing face-down onto a clean glass slide for observation.

Cell viability assay

The viability of Pt-nps treated cells was measured using CellTiter-Glo luminescent cell viability assay (Promega) following the manufacturer's instructions. This assay is a homogeneous method for determining the number of viable, metabolically-active cells in a culture based on the quantification of ATP concentration. The procedure involves addition of an equal volume of reagent to the medium in test wells, which in a single step generates a luminescent signal proportional to the concentration of ATP present in cells. The reagent contains detergents to break the cell membrane, causing ATP release into the medium and ATPase inhibitors to stabilize the released ATP. The assay is based on the conversion of luciferin to oxyluciferin by a recombinant luciferase in the presence of ATP. The observed luminescence is proportional to the quantity of ATP where viable cells produce more ATP than non-viable cells.

The experiments were performed in white, opaque-walled 96-well plates (Corning, Costar). Additional controls were included in the test to rule out autoluminescence and quenching by Pt-nps. For the ATP assay, 5000 cells were plated per well and incubated in 100 μl media overnight for the cells to adhere to the bottom of the well. Spent media was aspirated the next day and replaced with fresh media and the cells were treated with different concentrations of nanoparticles (25, 50, 100, 200, and 400 μg ml^{-1}) for 24, 48 and 72 h for all cell types. At respective time points, 100 μl of CellTiter-Glo viability assay pre-warmed to room temperature was added into each well and mixed properly. After 15 min, luminescence readings were measured using Tecan Infinite F200 micro-plate reader.

Apoptosis assay

Annexin-V staining was performed to differentiate apoptosis from necrotic cell death induced by Pt-nps. Annexin-V has a high affinity for phosphatidylserine, which is translocated from the

inner to the outer leaflet of the plasma membrane at an early stage of apoptosis. Its conjugation with the fluorescent probe FITC facilitates measurement by flow cytometry. Propidium iodide staining helps distinguish between apoptosis and necrosis due to difference in permeability of PI through the cell membranes of live and damaged cells. Pt-nps treated cells were harvested and washed twice in DPBS (Sigma-Aldrich) and stained (Annexin-V FITC apoptosis detection kit, Sigma-Aldrich) as per manufacturer's instructions. Flow cytometry was performed using Epics Altra (Beckman and Coulter) at an excitation wavelength of 490 nm and emission wavelength of 610 nm. Data was collected for 10 000 gated events and analyzed using Summit V4.3.02 software.

Statistical analysis

Statistical analyses of the values for all experiments are expressed as mean ± standard deviation of three independent experiments. The data were analyzed using *Student's t-test* (Microsoft Excel, Microsoft Corporation) where statistical significance was calculated for Pt-nps treated samples and also against untreated (control) cells. The data were subjected to unpaired one-tailed test and those with P values < 0.05 were considered as significant.

Results and discussion

Synthesis and purification of nanoparticles have been described in our previous papers.[11,12] For the synthesis of folic acid-capped platinum nanoparticles (Pt-FA), hexachloroplatinic acid and folic acid were mixed and stirred before adding sodium borohydride. As for PVP-capped platinum nanoparticles (Pt-PVP), the capping agent PVP was added immediately after the introduction of sodium borohydride.

A color change from yellow to light brown indicated the formation of Pt-PVP. The nanoparticles synthesized *via* the former approach were too small and could not be purified using centrifugation. Alternatively, switching the sequence of reagent addition produced a pellet after centrifugation which can be easily resuspended in water.

Uncapped platinum nanoparticles (Pt-nps) are insoluble in water and appeared as a black suspension after rigorous sonication. Such solutions are not stable for long periods and are unsuitable for biological studies. As shown in Fig. 2, both Pt-PVP and Pt-FA showed good dispersity in water with light brown and dark brown solutions, respectively. From the elemental analysis of the lyophilized particles, it is estimated that Pt-FA has a higher platinum content than Pt-PVP (18.24 wt% *vs.* 12.54 wt%).

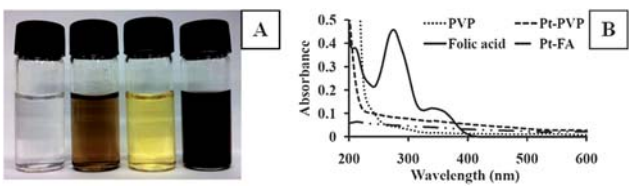

Fig. 2 Solutions of PVP, Pt-PVP, folic acid and Pt-FA at a concentration of 1 mg ml^{-1} in water. Folic acid was dissolved in phosphate buffer saline (PBS) to improve solubility (A). UV-visible spectrum of respective solutions (B). Purified Pt-nps did not show a peak in the spectrum.

Table 1 Chemical composition (in wt%) of Pt-PVP and Pt-FA

Element	Platinum	Carbon	Hydrogen	Nitrogen	Oxygen (estimate)
Pt-PVP	12.5	37.5	6.7	7.2	36.1
Pt-FA	18.2	5.35	3.1	1.2	72.15

Elemental analysis

From Table 1, it is apparent that the ratio of capping agent to platinum in Pt-PVP is high (high carbon to platinum ratio). On the contrary, low carbon content was observed for Pt-FA nanoparticles. Platinum content (12.5% *vs.* 18.2%) of both samples were comparable which enables a fair comparison between these two nanoparticles in cell viability testing. Oxygen content of Pt-FA was found to be higher than expected due to its hygroscopic nature.

Particle size and zeta potential measurements

TEM images revealed that Pt-nps form homogeneous colloids in water with no signs of agglomeration (Fig. 3A & 3B). This is important to make sure that individual nanoparticles are transported across cell membranes. The core size of Pt-PVP particles is in the range of 2–6 nm, while Pt-FA is larger with majority of particles in the range of 10–15 nm. Pt-PVP and Pt-FA are water dispersible owing to the hydrophilic capping agents which can prevent individual particles from aggregating. It should be noted that folic acid is more soluble in buffer solutions than in

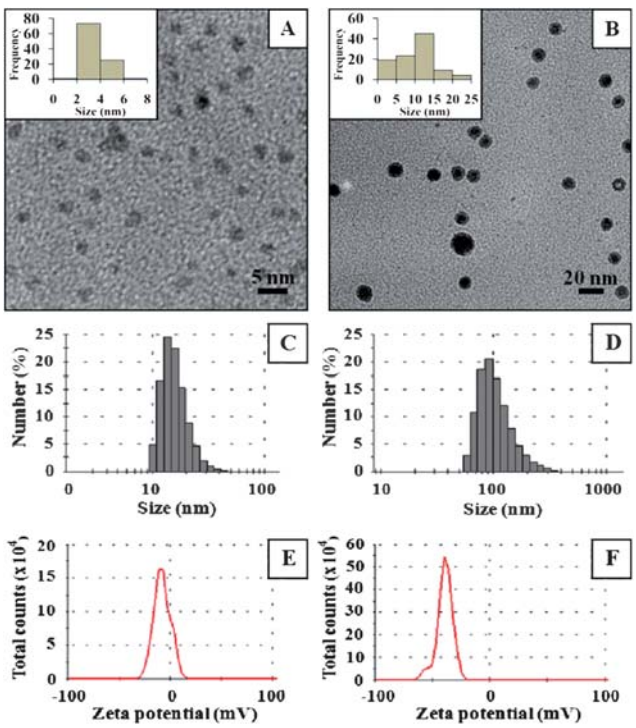

Fig. 3 TEM images of Pt-PVP (A) and Pt-FA (B). Insets represent size distribution of the nanoparticles. Data for the histogram were collected from 100 randomly picked particles. Dynamic light scattering histogram of Pt-PVP (C) and Pt-FA (D). Zeta potential distribution of Pt-PVP (E) and Pt-FA (F).

ultrapure water, which is preferred for cell viability assays. DLS measurements have showed that the mean hydrodynamic diameters were 13.5 nm and 91.3 nm for Pt-PVP and Pt-FA, respectively. PVP confers steric stabilization whereas folic acid gives an electrostatic stabilization. In contrast to Pt-PVP, Pt-FA has a highly-charged surface which is solvated by water molecules, which explains its increase in size after dissolving in water. TEM is used to determine the inner solid material diameter, while the hydrodynamic size distribution includes the solid particle, its organic layers (capping agents) and the hydration shell, which explains why DLS values are always larger.[13,14]

The zeta potential of Pt-PVP was at −8.0 mV while that of Pt-FA was at −40.5 mV. The highly-charged surface of Pt-FA arising from the ionization of acid functional groups resulted in a highly negative potential. Conversely, PVP is a neutral and hydrophilic polymer which stabilizes Pt-PVP through hydrophilic interactions with the solvent and therefore has a low surface potential.

CytoViva optical microscopy

Cell lines were grown on coverslips and treated with Pt-nps for 48 h before observation using CytoViva. Although the plasma membrane is vaguely observed in dark field microscopy, nuclear envelopes, cellular contents and organelles are distinct and brightly-illuminated. In all three cell types studied, untreated cells displayed a small number of bright, round circles which are evenly distributed throughout the cells (Fig. 4A, D and G). The identity of these bright specks (yellow arrows) could be organelles or transport vesicles (endosomes) which contain high concentrations of ions and proteins. Such bright spots should not be mistaken for Pt-nps aggregates (green arrows) which are non-circular (randomly-shaped). Pt-nps are too small to be observed directly under a light microscope and therefore the bright objects seen in these images are scattered light from nanoparticles.

Nanoparticles were able to enter the cytoplasm but not found inside the nucleus, which is consistent with literature findings.[15] With Pt-PVP treatment, cells appear to maintain their structural integrity as the membranes remained intact. In contrast, Pt-FA nanoparticles were found to enter cells more efficiently as indicated by more white specks. The plasma membranes became less distinct, especially in cancer cells. Fig. 4C and 4F show cell debris resulting from cell death.

Cell viability assay

A concentration and time-dependent study was conducted to find out their effects on cell viability. Commonly used cell

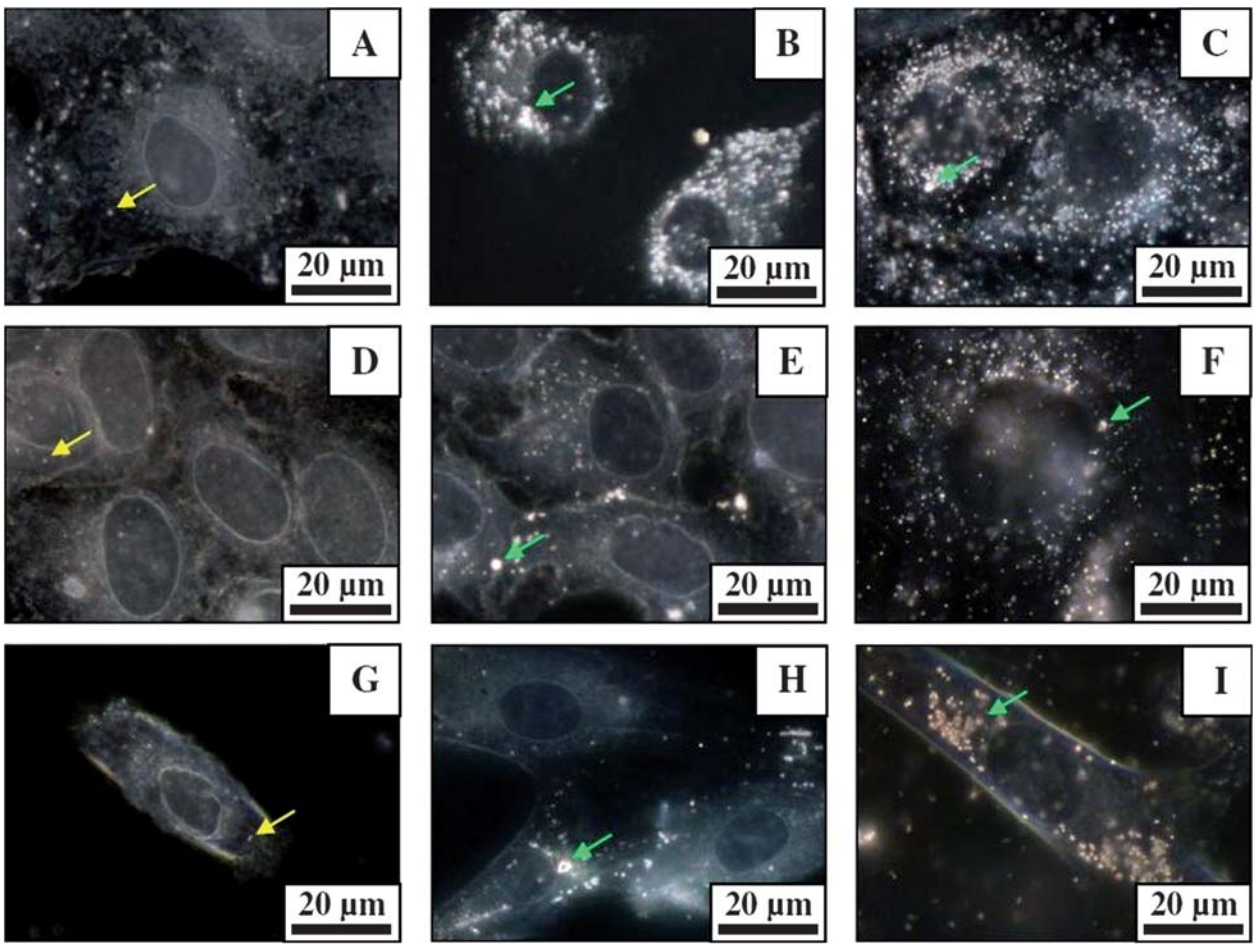

Fig. 4 Optical images of untreated (A), Pt-PVP treated (B), Pt-FA treated (C) HeLa cells. Untreated (D), Pt-PVP treated (E), Pt-FA treated (F) MCF7 cells. Untreated (G), Pt-PVP treated (H), Pt-FA treated (I) IMR90 cells. Concentration of Pt-nps = 100 μg ml^{-1}. Yellow arrows point to cellular components such as endosomes and lysosomes, while green arrows point to big Pt-nps aggregates.

viability assays are MTT (3-(4,5-dimethylthiazole-2-yl)-2,5-biphenyl tetrazolium bromide) or MTS (3-(4,5-dimethylthiazole-2-yl)-5-(3-carboxymethoxyphenyl)-2-(4-sulfophenyl)-2*H*-tetrazolium) which monitor the emission intensity of fluorescent dyes at specific wavelengths. A test substance, which might show similar optical properties to these dyes, can cause complications during the process of measurement. This is especially true when nanomaterials are being tested.[16,17] For example, silver and gold nanoparticles gave distinct UV absorption peaks due to surface plasmon resonance. Therefore, they give false-positive results when tested using the MTS or MTT assays.

The CellTiter-Glo luminescent cell viability assay is designed to monitor cytotoxicity as well as cell proliferation by measuring the number of viable cells in the culture medium. This assay measures the amount of ATP present, which is directly proportional to the number of viable cells. One advantage of this assay is the short waiting time (minutes) compared to MTS or MTT (four hours or more). A comparison between the ATP and the MTT assay revealed that the two assays gave different results when used to measure growth inhibition of various cancer drugs on the lung cancer cell line A549.[17] This is because the MTT assay measures the activity of dehydrogenases, while ATP concentration was measured in the case of ATP assay. Dying cells lose ATP faster than dehydrogenase activity, hence resulting in an over-estimation of cell viability when using the MTT assay. Owing to the fact that the ATP assay is more sensitive, it is used for our measurement.

The viability trends of Pt-PVP and Pt-FA treated cells were similar across different cell types. Generally, the viability of cells decreased with increasing Pt-nps concentration and with increasing exposure time from 24 h to 72 h (Fig. 5). Pt-PVP was comparatively non-toxic compared to Pt-FA. Although Pt-PVP was internalized by all cell lines as shown by dark field microscopy, the viability of cells was not affected until a high dose of 400 μg ml^{-1} was introduced, which reduced the viability of all cell types to less than 60% after 24 h. Increasing Pt-PVP concentration by eight-fold from 25 to 200 μg ml^{-1} did not reduce cell viability even after 72 h of exposure. On the other hand, Pt-FA is more toxic than Pt-PVP, especially to MCF7 breast cancer cells. Unlike Pt-PVP, the dose and time-dependency of Pt-FA are consistent across all cell types. At a low dose of 25 μg ml^{-1}, viability of HeLa, MCF7 and IMR90 dropped to 65%, 44%, and 43%, respectively, after 24 h, which is significantly lower than Pt-PVP. The inclusion of IMR90 amidst cancer cell lines allows a comparison of toxicity with normal cells. Little selectivity towards cancer cell lines over IMR90 was observed despite attaching folic acid on the Pt-nps

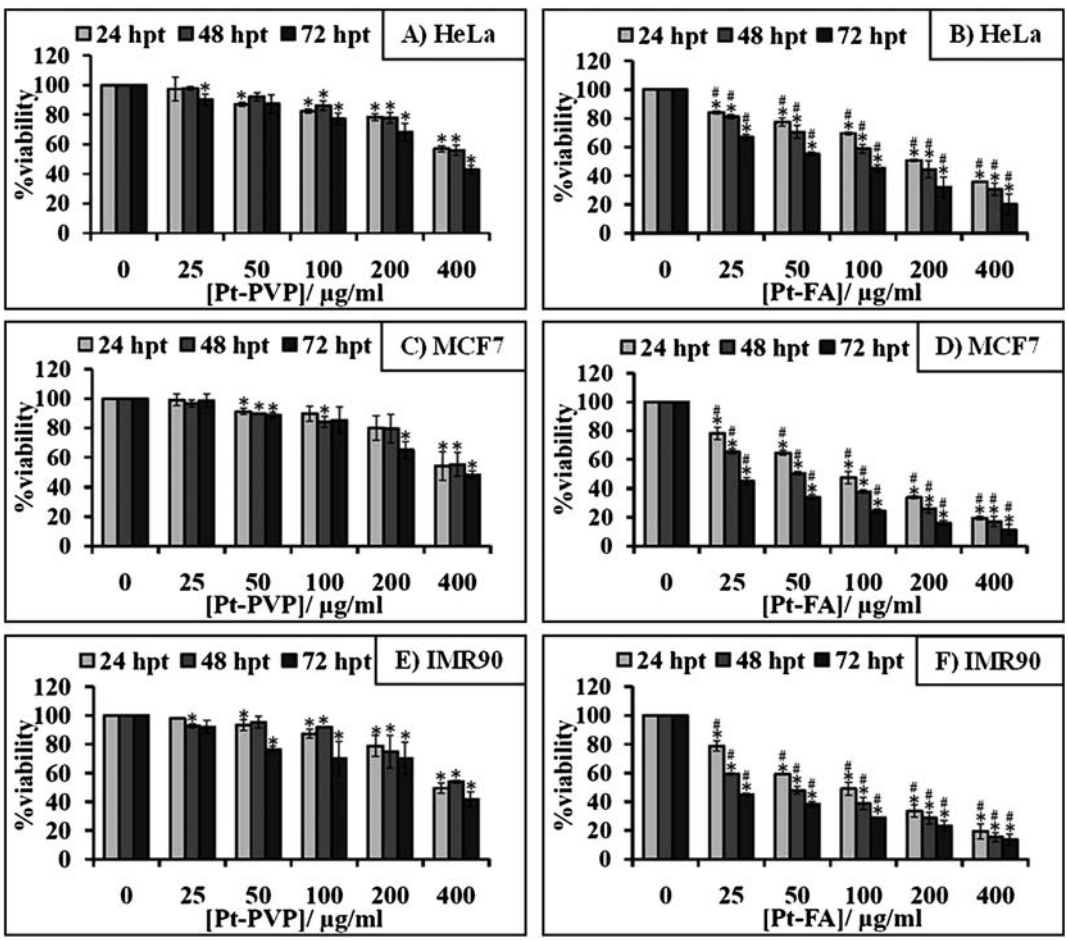

Fig. 5 Cell viability assays of HeLa (A, B), MCF7 (C, D), and IMR90 (E, F) after exposure to various concentrations of Pt-PVP and Pt-FA 24, 48 and 72 hpt. The *y*-axis represents the percentage of viable cells present in the treated sample after a certain time and the *x*-axis represents the final Pt-np concentration in culture. The values represent the mean ± standard deviation of three independent experiments; * denotes $P < 0.05$ with respect to the control group; # denotes $P < 0.05$ between Pt-PVP and Pt-FA using *Student's t test*.

surface *in vitro*. Folic acid was effective in directing Pt-nps into HeLa and MCF7 which over-expresses folate receptors as compared to nanoparticles capped with PVP. Although IMR90 does not over-express such receptors, it was affected by the toxic effects of platinum even at low doses of Pt-FA. However, under *in vivo* conditions, Pt-FA would be expected to deposit preferentially at the tumor site due to an enhanced permeability and retention effect (EPR) which improves the selectivity.[18–20] This is an advantage of nanodrug delivery systems as compared to conventional molecular cancer therapeutics such as cisplatin, which has a low circulation half-life.

The increase in toxicity of Pt-FA over Pt-PVP could be due to two reasons: (i) higher platinum content; and (ii) increased receptor-mediated endocytosis. The platinum content of Pt-FA is 18.2% as compared to 12.5% in Pt-PVP. Under slightly acidic conditions, Pt^0 can be converted to Pt^{2+},[21] which is believed to be responsible for the toxicity.[22]

$$Pt^0 \rightleftharpoons Pt^{2+} + 2e \qquad E^\circ = -1.18\ V^{23}$$

$$H_2O_2 + 2H^+ + 2e \rightleftharpoons 2H_2O \qquad E^\circ = +1.776\ V$$

$$Pt^0 + H_2O_2 + 2H^+ \rightleftharpoons Pt^{2+} + 2H_2O \qquad E^\circ_{cell} = +0.596\ V$$

These E° values were measured at standard temperature, pressure and concentration with respect to a standard hydrogen electrode, which may not reflect the true conditions in a living cell. However, a positive E° value signifies a spontaneous reaction. Gao *et al.* reported the use of $FePt@CoS_2$ yolk-shell nanocrystals as a potent agent to kill HeLa cells, where the FePt core was released from the shell and oxidized slowly during the process. Pt^{2+} ions can diffuse into the nucleus and mitochondria binding to DNA and leading to apoptosis of HeLa cells.[21,24]

Folic acid is a low molecular weight vitamin compound (B_9) which has been shown to be an effective tumor-targeting compound, especially in cancers such as breast, lung, kidney, ovarian and epithelial mouth cancers which over-express folate receptors.[20,25,26] Unlike antibodies or hormones-tagged particles which are shuttled to the lysosome for destruction, folic acid-tagged carriers are normally retained in an endocytic vesicle or released into the cytoplasm as folic acid is essential for cell functions.[19] Gold nanoparticles (Au-nps) with folic acid-linked PEG backbone and its efficiency *in vitro* have been widely reported.[19,27,28] Various other groups also reported the attachment of folic acid to other polymer backbones in nanocarriers.[29–33] This paper describes a simple but efficient way of directly attaching folic acid onto Pt-nps *via in situ* reduction of hexachloroplatinic acid in folic acid solution using sodium borohydride which does not require extensive organic synthesis or purification methods. The resulting nanoparticles were stable in water and cell medium. Also, the inherent toxicity of Pt-nps and the slow oxidation into Pt^{2+} ions as the source of anticancer activity have been incorporated into the design strategies. In fact, Pt-FA nanoparticles serve as carrier of folic acid and as a drug.

Other factors which can influence nanoparticles toxicity include size,[34–36] surface area, surface functionalities and charge.[36,37] In general, nanoparticle toxicity was found to increase with decreasing size due to the increase in reactive surface area for interaction with biological molecules or generation of reactive oxygen species. Waters *et al.* reported that changes in gene expression in murine macrophages correlated better with total surface area of silica nanoparticles rather than particle size or concentration.[38] Thevenot *et al.* tested TiO_2 nanoparticles with different surface chemistries in various murine cell lines and found that nanoparticles containing the amine functional group were more toxic than nanoparticles containing hydroxyl and carboxylic acid functional groups due to strong interaction with the negatively-charged cell membrane.[37] In fact, cationic liposomes are often used to deliver DNA with high transfection efficiencies.[39] Pt-FA is bigger (10–15 nm) and negatively-charged while Pt-PVP (2–6 nm) is smaller and neutral. Therefore, Pt-FA is expected to be less toxic than Pt-PVP. However, interaction with folate receptors enables Pt-FA to be internalized by cancer cells to exert its toxic effects.

Apoptosis assay

The apoptosis assay was carried out to assess the extent and mode of cell death upon exposure to Pt-nps. Stained cells were passed through the flow cytometer and the percentage of unstained cells (live cells), cells with red labels (took up the red propidium iodide stain, indicating necrosis), cells with green labels (took up the green signal from Annexin V-FITC, indicating early apoptosis) and finally cells which were dual-stained (late apoptosis), were generated from dot plots.

As expected, treatment of MCF7 with Pt-PVP did not change the percentage of viable cells and is comparable to our cell viability assay results using same Pt-nps concentration. Treatment with Pt-FA caused the percentage of live cells to drop by 8% and the combined percentage of cells entering late apoptosis and necrosis increased by 12%.

Interestingly, the response of IMR90 is entirely different from MCF7 with the same treatments. With Pt-PVP, there was no necrosis found in the control and the percentage of apoptotic cells observed was higher than the control by 47%. The percentage of early apoptotic cells stayed unchanged. However, with Pt-FA, the percentage of live cells decreased drastically to 14% of the total population and cells were found to undergo only necrosis. Therefore, the mechanism of uptake of these particles and its subsequent processing by IMR90 could be different from

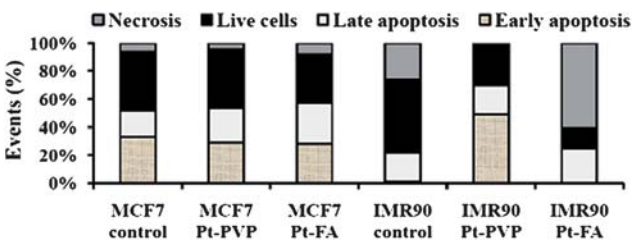

Fig. 6 Annexin-V staining of MCF7 and IMR90 treated with 100 μg ml^{-1} Pt-nps solution for 48 h. Cells stained with PI alone are necrotic, whereas cells stained with Annexin V-FITC alone represent early apoptosis. Cells at final stages of apoptosis take up both stains.

MCF7 cells. These results were consistent with the findings from Pan *et al.*, where they reported that 1.4 nm Au-nps caused necrosis in HeLa cells whereas 1.2 nm Au-nps resulted in cell death by apoptosis predominantly, despite both Au-nps having the same surface functionality.[34] While apoptosis is usually related to caspase activation,[40] calcium overload[41,42] or induced by death-inducing signals, necrosis is associated with loss of lysosomal membrane integrity.[43] The mechanism of cell death can be affected by small changes in particle size and functional groups found on the surface of nanoparticles. Such factors can have significant influence on membrane interaction, membrane damage, compartmentalization and processing of the nanoparticles after internalization.

Conclusion

PVP and folic acid-capped platinum nanoparticles have been synthesized to evaluate their bioactivities in commercial cell lines. The capping agents not only have an effect on the stability, shape and size distribution of the nanoparticles, but also in the uptake and toxicity of nanoparticles by live cells. At 25 μg ml^{-1}, viability of HeLa, MCF7 and IMR90 dropped significantly to 65%, 44%, and 43%, respectively, after 24 h of incubation with Pt-FA. The observed viabilities were >90% in the cases for Pt-PVP. Dark field optical microscope images also revealed increased accumulation of Pt-FA as compared to Pt-PVP, indicating the effectiveness of folic acid in receptor-mediated endocytosis. Pt-nps treatment caused an increase in proportions of MCF7 cells undergoing apoptosis, especially in the case of Pt-FA. For IMR90 cells, Pt-PVP treatment caused cells to undergo apoptosis, while Pt-FA caused necrosis to take place. This suggests that different capping agents caused dissimilar cellular component targeting. The inherent toxicity of platinum nanoparticles conferred an additional advantage to this nanocarrier by eliminating the need for attaching anticancer drugs to kill cancer cells.

Acknowledgements

Yiwei Teow would like to thank NGS for a PhD scholarship and all authors acknowledge technical support from Department of Chemistry, National University of Singapore. The authors also thank Ms P. V. AshaRani for her technical advice on the cell culture experiments performed.

References

1 L. Zhang, F. X. Gu, J. M. Chan, A. Z. Wang, R. S. Langer and O. C. Farokhzad, *Clin. Pharmacol. Ther.*, 2008, **83**, 761–769.
2 T. Murakami and K. Tsuchida, *Mini-Rev. Med. Chem.*, 2008, **8**, 175–183.
3 E. Rytting, K. A. Lentz, X. Q. Chen, F. Qian and S. Venkatesh, *AAPS J.*, 2005, **7**, E78–E105.
4 D. F. Veber, S. R. Johnson, H. Y. Cheng, B. R. Smith, K. W. Ward and K. D. Kopple, *J. Med. Chem.*, 2002, **45**, 2615–2623.
5 P. S. Low, *Mol. Pharmaceutics*, 2007, **4**, 629–630.
6 M. Chen, J. Falkner, W. H. Guo, J. Y. Zhang, C. Sayes and V. L. Colvin, *J. Colloid Interface Sci.*, 2005, **287**, 146–151.
7 S. D. Li and L. Huang, *Amer Chemical Soc*, 2007, 496–504.
8 J. Pan and S. S. Feng, *Biomaterials*, 2008, **29**, 2663–2672.
9 X. Q. Yang, Y. H. Chen, R. X. Yuan, G. H. Chen, E. Blanco, J. M. Gao and X. T. Shuai, *Polymer*, 2008, **49**, 3477–3485.
10 P. R. Van Rheenen, M. J. McKelvy and W. S. Glaunsinger, *J. Solid State Chem.*, 1987, **67**, 151–169.
11 P. V. Asharani, G. L. K. Mun, M. P. Hande and S. Valiyaveettil, *ACS Nano*, 2009, **3**, 279–290.
12 P. V. Asharani, Y. L. Wu, Z. Y. Gong and S. Valiyaveettil, *Nanotechnology*, 2008, **19**, 255102.
13 B. M. Barth, R. Sharma, E. I. Altinoglu, T. T. Morgan, S. S. Shanmugavelandy, J. M. Kaiser, C. McGovern, G. L. Matters, J. P. Smith, M. Kester and J. H. Adair, *ACS Nano*, 2010, **4**, 1279–1287.
14 S. Kittler, C. Greulich, J. S. Gebauer, J. Diendorf, L. Treuel, L. Ruiz, J. M. Gonzalez-Calbet, M. Vallet-Regi, R. Zellner, M. Koller and M. Epple, *J. Mater. Chem.*, 2010, **20**, 512–518.
15 T. Komatsu, M. Tabata, M. Kubo-Irie, T. Shimizu, K. Suzuki, Y. Nihei and K. Takeda, *Toxicol. in Vitro*, 2008, **22**, 1825–1831.
16 S. H. Doak, S. M. Griffiths, B. Manshian, N. Singh, P. M. Williams, A. P. Brown and G. J. S. Jenkins, *Mutagenesis*, 2009, **24**, 285–293.
17 E. Ulukaya, F. Ozdikicioglu, A. Y. Oral and M. Demirci, *Toxicol. in Vitro*, 2008, **22**, 232–239.
18 T. M. Allen and P. R. Cullis, *Science*, 2004, **303**, 1818–1822.
19 J. D. Byrne, T. Betancourt and L. Brannon-Peppas, *Adv. Drug Delivery Rev.*, 2008, **60**, 1615–1626.
20 D. Peer, J. M. Karp, S. Hong, O. C. FaroKhzad, R. Margalit and R. Langer, *Nat. Nanotechnol.*, 2007, **2**, 751–760.
21 J. H. Gao, G. L. Liang, J. S. Cheung, Y. Pan, Y. Kuang, F. Zhao, B. Zhang, X. X. Zhang, E. X. Wu and B. Xu, *J. Am. Chem. Soc.*, 2008, **130**, 11828–11833.
22 P. V. Asharani, N. Xinyi, M. P. Hande and S. Valiyaveettil, *Nanomedicine*, 2010, **5**, 51–64.
23 D. R. Lide, *CRC Handbook of Chemistry and Physics*, CRC Press, 2000.
24 J. H. Gao, G. L. Liang, B. Zhang, Y. Kuang, X. X. Zhang and B. Xu, *J. Am. Chem. Soc.*, 2007, **129**, 1428–1433.
25 N. Wiradharma, Y. Zhang, S. Venkataraman, J. L. Hedrick and Y. Y. Yang, *Nano Today*, 2009, **4**, 302–317.
26 J. M. Rosenholm, E. Peuhu, J. E. Eriksson, C. Sahlgren and M. Linden, *Nano Lett.*, 2009, **9**, 3308–3311.
27 E. Gullotti and Y. Yeo, *Mol. Pharmaceutics*, 2009, **6**, 1041–1051.
28 C. R. Patra, R. Verma, S. Kumar, P. R. Greipp, D. Mukhopadhyay and P. Mukherjee, *J. Biomed. Nanotechnol.*, 2008, **4**, 499–507.
29 T. Yoshida, N. Oide, T. Sakamoto, S. Yotsumoto, Y. Negishi, S. Tsuchiya and Y. Aramaki, *J. Controlled Release*, 2006, **111**, 325–332.
30 J. You, X. Li, F. de Cui, Y. Z. Du, H. Yuan and F. Q. Hu, *Nanotechnology*, 2008, **19**, 9.
31 E. K. Park, S. Y. Kim, S. B. Lee and Y. M. Lee, *J. Controlled Release*, 2005, **109**, 158–168.
32 R. Bhattacharya, C. R. Patra, A. Earl, S. F. Wang, A. Katarya, L. Lu, J. N. Kizhakkedathu, M. J. Yaszemski, P. R. Greipp, D. Mukhopadhyay and P. Mukherjee, *Nanomed.: Nanotechnol., Biol. Med.*, 2007, **3**, 224–238.
33 J. Pan and S. S. Feng, *Biomaterials*, 2009, **30**, 1176–1183.
34 Y. Pan, S. Neuss, A. Leifert, M. Fischler, F. Wen, U. Simon, G. Schmid, W. Brandau and W. Jahnen-Dechent, *Small*, 2007, **3**, 1941–1949.
35 S. M. Hussain, K. L. Hess, J. M. Gearhart, K. T. Geiss and J. J. Schlager, *Toxicol. in Vitro*, 2005, **19**, 975–983.
36 C. Carlson, S. M. Hussain, A. M. Schrand, L. K. Braydich-Stolle, K. L. Hess, R. L. Jones and J. J. Schlager, *J. Phys. Chem. B*, 2008, **112**, 13608–13619.
37 P. Thevenot, J. Cho, D. Wavhal, R. B. Timmons and L. P. Tang, *Nanomed.: Nanotechnol., Biol. Med.*, 2008, **4**, 226–236.
38 K. M. Waters, L. M. Masiello, R. C. Zangar, N. J. Karin, R. D. Quesenberry, S. Bandyopadhyay, J. G. Teeguarden, J. G. Pounds and B. D. Thrall, *Toxicol. Sci.*, 2009, **107**, 553–569.
39 V. P. Torchilin, *Adv. Drug Delivery Rev.*, 2006, **58**, 1532–1555.
40 J. E. Chipuk and D. R. Green, *Nat. Rev. Mol. Cell Biol.*, 2005, **6**, 268–275.
41 T. Ozaki, T. Yamashita and S. Ishiguro, *Biochim. Biophys. Acta, Mol. Cell Res.*, 2009, **1793**, 1848–1859.
42 A. Jahani-Asl, M. Germain and R. S. Slack, *Biochim. Biophys. Acta-Mol. Basis Dis.*, 2010, **1802**, 162–166.
43 R. Castino, M. Demoz and C. Isidoro, *J. Mol. Recognit.*, 2003, **16**, 337–348.